BASIC SCIENCE

Nanomedicine: Nanotechnology, Biology, and Medicine
21 (2019) 102073

Original Article

nanomedjournal.com

Preferential uptake of chitosan-coated PLGA nanoparticles by primary human antigen presenting cells

Verónica Durán, M.Sc[a,1], Hanzey Yasar, PhD[b,c,1], Jennifer Becker, PhD[a], Durairaj Thiyagarajan, PhD[b,c], Brigitta Loretz, PhD[b,c], Ulrich Kalinke, Professor[a,d,*], Claus-Michael Lehr, Professor[b,c,**]

[a]*Institute for Experimental Infection Research, TWINCORE, Centre for Experimental and Clinical Infection Research, a joint venture between the Hannover Medical School and the Helmholtz Centre for Infection Research, Hannover, Germany*

[b]*Department of Pharmacy, Saarland University, Saarbrücken, Germany*

[c]*Helmholtz-Institute for Pharmaceutical Research Saarland (HIPS) - Helmholtz Center for Infection Research (HZI) Department of Drug Delivery (DDEL), Saarbrücken, Germany*

[d]*Cluster of Excellence - Resolving Infection Susceptibility (RESIST), Hannover Medical School, Hannover, Germany*

Revised 2 July 2019

Abstract

Biodegradable polymeric nanoparticles (NP) made from poly (lactid-co-glycolide) acid (PLGA) and chitosan (CS) hold promise as innovative formulations for targeted delivery. Since interactions of such NP with primary human immune cells have not been characterized, yet, here we assessed the effect of PLGA or CS-PLGA NP treatment on human peripheral blood mononuclear cells (PBMC), as well as on monocyte-derived DC (moDC). Amongst PBMC, antigen presenting cells (APC) showed higher uptake of both NP preparations than lymphocytes. Furthermore, moDC internalized CS-PLGA NP more efficiently than PLGA NP, presumably because of receptor-mediated endocytosis. Consequently, CS-PLGA NP were delivered mostly to endosomal compartments, whereas PLGA NP primarily ended up in lysosomes. Thus, CS-PLGA NP confer enhanced delivery to endosomal compartments of APC, offering new therapeutic options to either induce or modulate APC function and to inhibit pathogens that preferentially infect APC.

Key words: Nanoparticles; PLGA NP; Chitosan-PLGA NP; PBMC; Monocyte-derived DC; Intracellular trafficking

Over the past few decades, nanoparticles (NP) gained increased attention as an innovative approach to improve drug delivery. In particular for the treatment of diseases such as infections and cancer, NP formulations hold promise as new strategies.[1] Due to their physicochemical properties that facilitate interactions with biological systems,[2] their morphological structure that allows for efficient cellular uptake,[3] and the option to functionalize their surface,[4] NP formulations represent a versatile tool to improve delivery of a whole variety of cargos to their preferred site of action. As such, NP have been widely studied for vaccine formulations,[5] cancer treatment,[6] gene therapeutic purposes,[7] immunotherapies,[8] and diagnostics.[9] Tuning their physicochemical properties resulted in enhanced crossing of biological barriers and increased bioavailability. However, also safety concerns were raised against NP.[10,11] It has been reported that NP may cause adverse effects when coming into contact with human immune cells.[12,13] This sets strict requirements for the selection of materials and excipients when designing NP. We focused on the analysis of two delivery systems composed of poly (lactid-co-glycolide) acid (PLGA). Such anionic PLGA NP can be subjected to chitosan-surface

Funding: This study was partially supported by the Helmholtz "Zukunftsthema Immunology und Inflammation" [ZT-0027] and by the Deutsche Forschungsgemeinschaft (DFG, Joint French-German Project cGAS-VAV [406922110]) to U.K.

Acknowledgments: The authors would like to thank Dr. Chiara De Rossi for support in performing TEM visualization studies. We thank Dr. Chintan Chhatbar for scientific discussion.

Conflict of interest: The authors declare no conflict of interest

*Correspondence to: U. Kalinke, PhD, Institute for Experimental Infection Research, TWINCORE, Center for Experimental and Clinical Infection Research, a joint venture between the Hannover Medical School and the Helmholtz Centre for Infection Research, Hannover, Germany.

**Correspondence to: C-M Lehr, PhD, Helmholtz-Institute for Pharmaceutical Research Saarland (HIPS) - Helmholtz Center for Infection Research (HZI) Department of Drug Delivery (DDEL), Saarbrücken, Germany.

E-mail addresses: Ulrich.Kalinke@twincore.de, (U. Kalinke), Claus-Michael.Lehr@helmholtz-hzi.de. (C.-M. Lehr).

[1] equally contributing authors

https://doi.org/10.1016/j.nano.2019.102073

Please cite this article as: Durán V, et al, Preferential uptake of chitosan-coated PLGA nanoparticles by primary human antigen presenting cells. *Nanomedicine: NBM* 2019;21:102073, https://doi.org/10.1016/j.nano.2019.102073

coating, thus resulting in cationic chitosan-coated PLGA (CS-PLGA) NP.[14,15] These polymers are biodegradable and biocompatible and therefore were already approved by regulatory authorities as pharmaceutically safe materials for clinical and cosmetic use.[16,17]

PLGA and CS-PLGA NP have been successfully exploited in vaccination via the transfollicular route.[15] Interestingly, this vaccination approach induced immune responses against the model antigen ovalbumin only when an adjuvant was added.[18] Further studies used CS-PLGA NP for messenger RNA (mRNA) delivery upon intravenous administration in mice.[19,20]

The delivery potential of NP to antigen presenting cells (APC) has gained increased interest due to the function of APC as first line defense against pathogens as well as for their key role in inducing antigen-specific immune responses.[21] NP should allow for APC-selective delivery of immune-modulating molecules as well as antimicrobial compounds without inducing adverse immune reactions. Here, we studied the interaction of PLGA and CS-PLGA NP with primary human immune cells. Importantly, cells derived from human PBMC more closely reflect the pathophysiological state of immune cells in humans than tumor cell lines. Hence, (i) we prepared anionic PLGA and cationic CS-PLGA NP and fluorescently labeled them for cellular visualization purposes and (ii) we tested the uptake of both NP preparations by different immune cell subsets contained within human PBMC. (iii) To more specifically study NP uptake by APC, we isolated monocytes from PBMC, differentiated them to monocyte-derived dendritic cells (moDC), and tested the uptake and cytotoxic effect following NP treatment. (iv) Furthermore, we studied the immunological safety profile of NP treatment by analyzing the activation status of moDC upon NP treatment, and (v) we analyzed to which subcellular DC compartments the NP travel after cellular uptake. In brief, these studies indicated that in particular CS-PLGA NP are a versatile tool to selectively deliver drugs to APC into endosomal compartments.

Methods

Preparation and characterization of PLGA and chitosan-coated PLGA nanoparticles

For the production of plain (anionic) PLGA or chitosan-coated (cationic) CS-PLGA NP, a modified double-emulsion method was used as described previously.[15] In brief, 50 mg of PLGA (50:50; Resomer RG 503H, Evonik Industries AG, Darmstadt, Germany) was dissolved in ethyl acetate. Then 400 μl of milli-Q water (Merck Millipore, Billerica, MA) was added to the PLGA organic phase. This solution was sonicated with an ultrasound device (Branson Ultrasonic Corporation, USA) for 30 s at a 30% amplitude. Next, a solution of 2% (w/V) polyvinyl alcohol (PVA; Mowiol® 4–88, Sigma-Aldrich, Darmstadt, Germany) was prepared with milli-Q water. A volume of 4 ml PVA solution was applied to the initial PLGA solution and sonicated at the above settings. After continuous stirring overnight, the solution was purified by using a dialysis membrane (MWCO 1 kDa, Spectrum Labs, CA, USA) to obtain a final solution of 2 mg/ml PLGA NP. Similarly, chitosan-coated PLGA NP were produced by supplementing the PVA solution with 0.2% (w/v) chitosan (Protasan UP CL 113, FMC Biopolymer AS Novamatrix, Sandvika, Norway). For visualization purposes, the NP were fluorescently labeled by covalently coupling fluoresceinamine (FA; Sigma-Aldrich, Darmstadt, Germany).[22]

All NP used in this study were thoroughly characterized for their quality attributes. Using dynamic light scattering (Zetasizer, Malvern Instruments, Malvern, UK), three colloidal properties were analyzed: the hydrodynamic size, the polydispersity index (PDI) and the ζ-potential. The morphology of NP was determined by using transmission electron microscopy (TEM; JEOL JEM 2011, St. Andrews, UK), as reported previously.[22] All excipients, including materials and polymers, as well as the produced NP were in house tested for the absence of endotoxins by using the EndoLISA® detection assay (Hyglos GmbH, Bernried am Starnberger See, Germany).

Isolation of primary human immune cells

Human PBMC were isolated from buffy coats of healthy blood donors provided by the Blutbank Springe (Germany) using Ficoll density gradient centrifugation (Biocoll, Biochrom AG). CD14-positive monocytes were isolated by MACS selection (Miltenyi). To differentiate monocyte-derived dendritic cells (moDC), purified monocytes were cultivated for 5 days in serum-free DC CellGro® medium (CellGenix, Freiburg, Germany) enriched with 1000 U/ml GM-CSF (granulocyte macrophage-colony stimulating factor, CellGenix) and 1000 U/ml IL-4 (CellGenix).

Flow cytometry analysis

1×10^6 PBMC were immunolabeled with anti-CD3-PerCP (UCHT1, Biolegend), anti-CD14-PacBlue (M5E2, Biolegend), anti-CD19-Amcyan (HIB19, BD Biosciences), and anti-HLA-DR-APC-Cy7 (L243; Biolegend) for 15 min at 4 °C. For immune activation studies, 5×10^5 moDC cells were harvested and immunolabeled with anti-CD40-PE (5C3, Biolegend), anti-CD86-PacBlue (IT2.2, Biolegend), anti-HLA-AB-PeCy5 (W6/32, BD Biosciences), anti HLA-DR-APC-Cy7 (L243, Biolegend), anti-CD11c-PeCy7 (3.9, Biolegend) and anti-CD206-APC (15–2; Biolegend). Unspecific immunolabeling of PBMC and moDC was blocked by the addition of 10% Gamunex (Grifols Deutschland GmbH, Frankfurt am Main, Germany). Data were acquired on a LSRII flow cytometer (BD Biosciences) and analyzed using the FlowJo software (Tree Star).

Nanoparticle binding and uptake studies

To analyze NP uptake, 60 μg/ml of FA-PLGA or CS-FA-PLGA NP were added to 1×10^6 PBMC and incubated either at 4 °C or 37 °C. Cells were harvested, immunolabeled and NP-derived FA fluorescence was assessed by flow cytometry. Binding of NP to the cell surface was determined as the percentage of FA positive cells after incubation at 4 °C. Net uptake of NP was calculated by subtracting the NP binding from the percentage of FA positive cells observed at 37 °C. For uptake inhibition studies, moDC were incubated for 30 min with the inhibitors cytochalasin D, dynasore and filipin (Sigma-Aldrich,

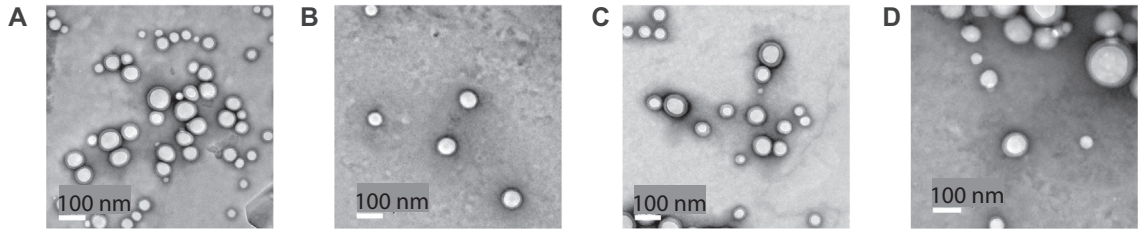

E

Nanoparticle	Size (nm)	PDI	ζ-potential (mV)
PLGA	127 ± 12	0.12 ± 0.07	-18.4 ± 3.8
FA-PLGA	162 ± 34	0.05 ± 0.03	-16.3 ± 5.6
CS-PLGA	151 ± 20	0.17 ± 0.08	26.8 ± 1.5
CS-FA-PLGA	183 ± 26	0.09 ± 0.00	13.1 ± 6.2

Figure 1. **Morphological and physicochemical characterization of PLGA and chitosan-coated PLGA nanoparticles.** Transmission electron micrographs of **(A)** non-labeled PLGA NP, **(B)** FA-PLGA NP, **(C)** non-labeled CS-PLGA NP and **(D)** CS-FA-PLGA NP. **(E)** The NP preparations were characterized by dynamic light scattering (DLS) for their size, polydispersity index (PDI) and ζ-potential. Data presented as mean ± SD *(n = 3)*.

Darmstadt, Germany) prior to NP treatment. Cytochalasin D inhibits actin-polymerization and thus mainly blocks macropinocytosis, dynasore mostly blocks clathrin-mediated endocytosis, and filipin blocks caveolae-mediated endocytosis. After exposure to FA-labeled NP, the mean fluorescence intensity (MFI) of moDC was determined by flow cytometry and the fold reduction of fluorescence relative to controls was calculated as a measure of inhibition of NP uptake.

Confocal fluorescence microscopy

For confocal imaging, moDC were seeded in coverslip-bottom LabTeK® culture chambers (Sigma-Aldrich, Darmstadt, Germany) during the five days of moDC differentiation. After NP treatment, cells were fixed with 3% paraformaldehyde for 10 min at room temperature, washed three times with PBS and blocked with glycine-containing blocking buffer for 1 hour. Cells were washed again three times with PBS and incubated with primary antibodies of interest for 24 hours at 4 °C. After PBS washing, fluorophore-conjugated secondary antibodies were added and the samples were incubated for 2 hours at room temperature. Finally, DAPI was added for nuclear staining, cells were washed and mounted with DAKO fluorescent mounting medium. Confocal microscopy was then performed with the Olympus FV1000-IX81 laser-scanning microscope using the 60x oil immersion objective, NA 1.35.

Statistical analysis

All data analyses were performed using the GraphPad Prism Software (La Jolla CA).

To compare matched samples, two tailed Wilcoxon test was used with a p-value <0.05 set as statistically significant and for colocalization studies, a two-way ANOVA was performed with a p-value <0.05 set as significant. All measurements were performed at least 3 times. For uptake inhibition studies, the non-parametric Friedman's test was used with a p-value <0.05 set as significant.

Results

Production and characterization of PLGA and chitosan-coated PLGA nanoparticles

For this study anionic PLGA and cationic chitosan-coated PLGA NP were generated as described earlier.[13,14] As even minor variations in the physicochemical properties of NP preparations can influence their functionality and bioavailability, we characterized the morphology, the size, the polydispersity index (PDI), the ζ-potential, the endotoxin content, and the stability under cell culture conditions of NP preparations used in this study. PLGA and CS-PLGA NP with and without FA-labeling revealed a smooth and evenly shaped spherical morphology (Figure 1, *A–D*), with a hydrodynamic size of approx. 130 nm for PLGA and 150 nm for CS-PLGA NP (Figure 1, *E*). Consistent results were obtained in the analysis of CS-PLGA NP by different microscopy techniques, including cryo-electron microscopy.[23] Both NP preparations had a monodisperse particle-size distribution as indicated by a PDI of approx. 0.1. PLGA NP showed an anionic surface charge with a ζ-potential of approx. -18 mV, whereas CS-PLGA NP were cationic with a ζ-potential of approx. +26 mV (Figure 1, *E* and Supplementary Table 1). FA-labeling only moderately increased the size of both NP preparations and reduced the ζ-potential of CS-PLGA NP from +26 to +13 mV. Nevertheless, non-labeled and FA-labeled CS-PLGA NP had a positive charge. As in studies with primary human immune cells the purity of the analyzed NP preparations is of key relevance, only pharmaceutical grade materials were used to generate NP preparations. Additionally, each excipient used for NP production as well as the final NP preparations were tested endotoxin free (Supplementary Table 2). The stability and aggregation behavior of

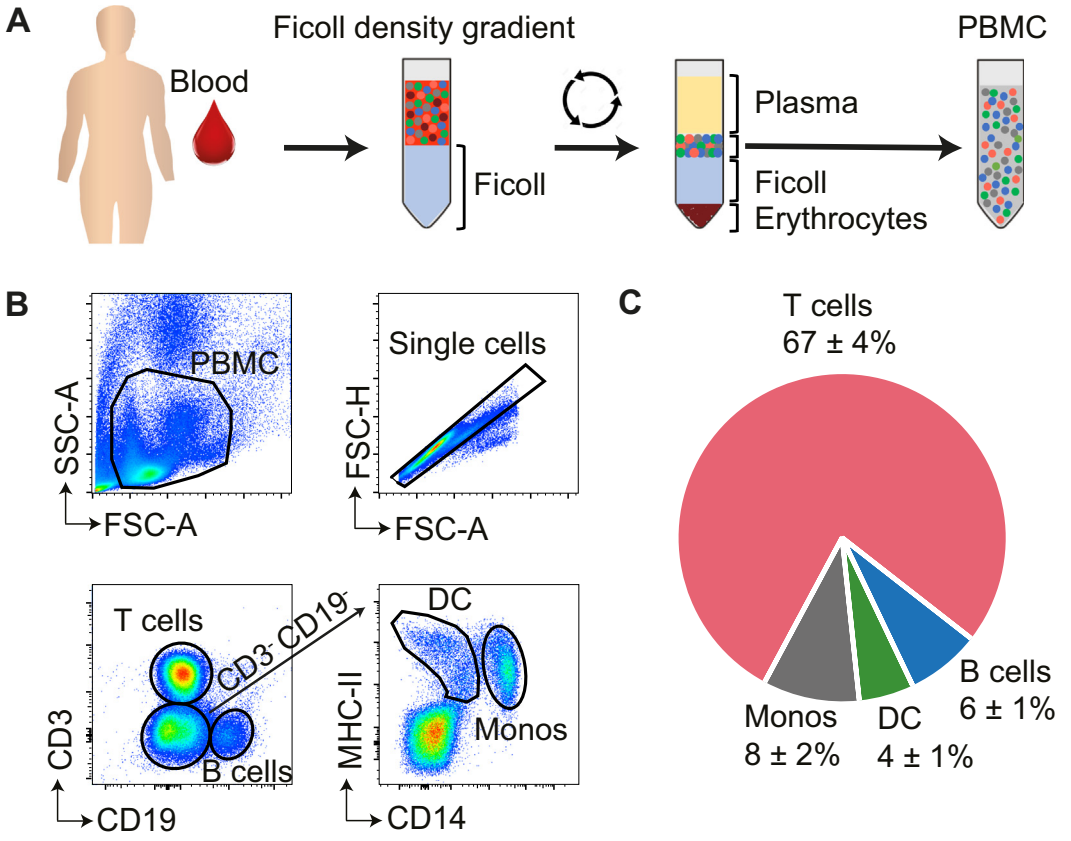

Figure 2. **Characterization of immune cell subsets in human PBMC. (A)** Blood was drawn from healthy donors and human PBMC were isolated by Ficoll density gradient centrifugation. **(B)** Human PBMC were immunolabeled with fluorescent-coupled antibodies specific for CD3, CD19, MHC-II, and CD14. $CD3^+CD19^-$ T cells, $CD3^-CD19^+$ B cells, $CD3^-CD19^-MHCII^+CD14^+$ monocytes (monos) and $CD3^-CD19^-MHCII^+CD14^-$ dendritic cells (DC) were gated as indicated for one representative donor. **(C)** Cell subset distribution amongst PBMC from 11 healthy donors. Values indicate mean percentage ± SD.

PLGA and CS-PLGA NP was tested after long-term storage at 4 °C, but no significant differences were observed, neither in size, PDI, or ζ-potential (Supplementary Table 3). Furthermore, both NP preparations were incubated in fresh CellGro® medium or in medium harvested after 5 days of moDC culture (conditioned medium) and the hydrodynamic size as well as the PDI were measured. PLGA and CS-PLGA NP showed a similar size and PDI after incubation in PBS or fresh medium. In contrast, following incubation in conditioned medium both NP showed moderately increased size and PDI (Supplementary Figure 1). Therefore, a medium exchange was performed prior to NP treatment of cells in the following in vitro experiments.

Among PBMC, antigen presenting cells show enhanced uptake of PLGA and chitosan-coated PLGA nanoparticles

To study NP uptake by primary human immune cells, blood samples were drawn from healthy donors and PBMC were isolated by Ficoll density gradient centrifugation (Figure 2, *A*). To determine the immune cell subset distribution amongst PBMC, cells prepared from 11 different donors were immunolabeled with fluorescent-coupled antibodies directed against CD3, CD19, MHC-II, and CD14, and samples were analyzed by flow cytometry. Amongst single cells, T cells were defined as $CD3^+CD19^-$ cells and B cells as $CD19^+CD3^-$ cells, whereas the $CD3^-CD19^-$ population was further dissected in $MHC\text{-}II^+CD14^+$ monocytes and $MHC\text{-}II^+CD14^-$ dendritic cells (DC) (Figure 2, *B*). This analysis revealed that PBMC comprise approx. 67% T cells, 6% B cells, 4% DC, and 8% monocytes (Figure 2, *C*).

To investigate the kinetics of NP uptake, PBMC were treated with 60 μg/ml of FA-PLGA or CS-FA-PLGA NP and after incubation at 37 °C for the indicated times, cells were harvested, immunolabeled as described above, and the percentages of FA positive cells were determined by flow cytometry. Incubation at 4 °C was performed as a control to determine the FA signal derived from binding of nanoparticles to the cell surface (Supplementary Figure 2). Under such conditions, T cells did not show abundant percentages of FA positive cells, neither upon treatment with FA-PLGA nor CS-FA-PLGA NP, and not even after 4 h of incubation (Figure 3, *A*). Furthermore, less than 20% of B cells were FA positive after 4 h treatment with FA-PLGA NP, but not after treatment with CS-FA-PLGA NP (Figure 3, *B*). In contrast, DC and monocytes showed increased fluorescence already after 15 min of incubation with CS-FA-PLGA NP, but not after FA-PLGA NP treatment (Figure 3, *C and D*). After prolonged incubation of up to 4 h, approx. 40% of the DC were FA positive upon treatment with CS-FA-PLGA NP, while only

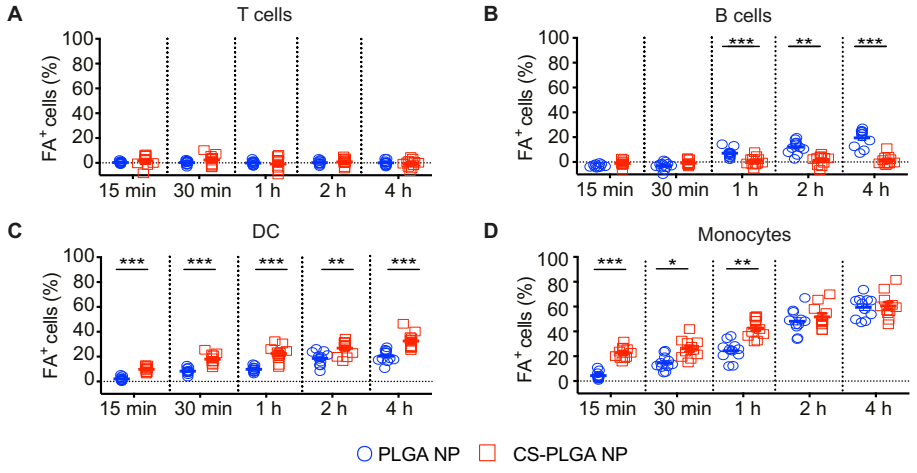

Figure 3. **FA-PLGA and CS-FA-PLGA nanoparticles are preferentially taken up by APC in human PBMC.** PBMC prepared as described in Fig. 2 were treated with 60 μg/ml of FA-PLGA or CS-FA-PLGA NP at 37 °C for the indicated times. Percentages of FA positive cells were determined for **(A)** T cells, **(B)** B cells, **(C)** DC and **(D)** monocytes. Values were normalized to the fluorescence signal detected after incubation at 4 °C (Supplementary Figure 1). Error bars indicate mean ± SEM (two-tailed Wilcoxon test, ***$P \leq 0.0010$, **$P \leq 0.0068$, *$P \leq 0.0137$, n = 11).

20% were positive upon FA-PLGA NP treatment (Figure 3, *C*). Interestingly, after 4 h of incubation, approx. 60% of the monocytes were FA positive, irrespective of whether the PBMC were treated with FA-PLGA or CS-FA-PLGA NP (Figure 3, *D*). Thus, upon treatment of PBMC with FA-PLGA or CS-FA-PLGA NP, primarily myeloid cells including DC and monocytes, but not lymphocytes, showed enhanced NP uptake. Of note, monocytes took up NP even more efficiently than DC and after short incubation times, both myeloid cell subsets showed enhanced uptake of CS-FA-PLGA NP when compared with FA-PLGA NP.

Chitosan-coated PLGA nanoparticles are effectively internalized by monocyte-derived dendritic cells and do not show toxic effects

As DC are of key relevance for the induction and regulation of antigen-specific immune responses and thus constitute an interesting pharmacological target, the delivery of NP in DC was studied in greater detail. To this end, $CD14^+$ cells were isolated from PBMC by magnetic cell sorting and further differentiated to monocyte-derived dendritic cells (moDC) (Figure 4, *A*). To analyze the effect of NP treatment on cell viability, moDC were exposed to increasing concentrations of FA-PLGA or CS-FA-PLGA NP and the percentage of dead cells was quantified using the Zombie Aqua™ dye. These experiments indicated that up to a concentration of 100 μg/ml, only low toxicity was detected for both NP. At the highest concentration of 600 μg/ml, approx. 20% and 40% of the moDC were dead upon treatment with FA-PLGA and CS-FA-PLGA NP, respectively (Supplementary Figure. 3). Therefore, moDC were exposed to 60 μg/ml of either type of NP preparation and the percentage of FA positive cells was determined by flow cytometry. Incubation with CS-FA-PLGA NP resulted in significantly increased percentages of FA positive cells at all the tested time points, with approx. 70% FA positive cells after 24 h of incubation. In contrast, treatment with FA-PLGA NP resulted only in approx. 30% FA positive cells after 24 h of incubation (Figure 4, *C*). These results demonstrated that CS-FA-PLGA NP are more efficiently taken up by moDC than FA-PLGA NP.

FA-labeled PLGA nanoparticles are primarily taken up by actin-dependent endocytosis, while chitosan-coated PLGA nanoparticles enter moDC mainly by clathrin-mediated endocytosis

To address the cellular pathway by which NP enter into moDC, we pre-incubated cells with increasing concentrations of the pharmacological inhibitors cytochalasin D, dynasore and filipin and then measured the fold reduction of FA-PLGA or CS-FA-PLGA NP uptake relative to NP only controls (Figure 5). Upon treatment with cytochalasin D, which inhibits actin-polymerization and thus mainly blocks macropinocytosis,[24] we observed a 0.7-fold reduction in the uptake of FA-PLGA NP, even at the lowest concentration (Figure 5, *A* and *B* upper panel). In contrast, uptake of CS-FA-PLGA NP was only significantly decreased after preincubation with 20 μM cytochalasin D, with a 0.4-fold reduction relative to the only NP control (Figure 5, *A* and *B* lower panel). To block clathrin-mediated endocytosis we used the dynamin inhibitor dynasore.[25] This inhibitor did not significantly change the uptake of FA-PLGA NP, not even at the highest concentrations, but a 0.4-fold reduction in the uptake of CS-FA-PLGA NP was detected after treatment with 50 μM and 100 μM dynasore. Finally, we used filipin to inhibit caveolae-mediated endocytosis,[26] but we did not observe any significant change in the uptake of neither FA-PLGA nor CS-FA-PLGA NP (Figure 5, *B*). Thus, our results indicate that the predominant uptake mechanism of FA-PLGA NP in moDC is macropinocytosis, while in the case of CS-FA-PLGA NP clathrin-mediated endocytosis seems to be the preferred mechanism.

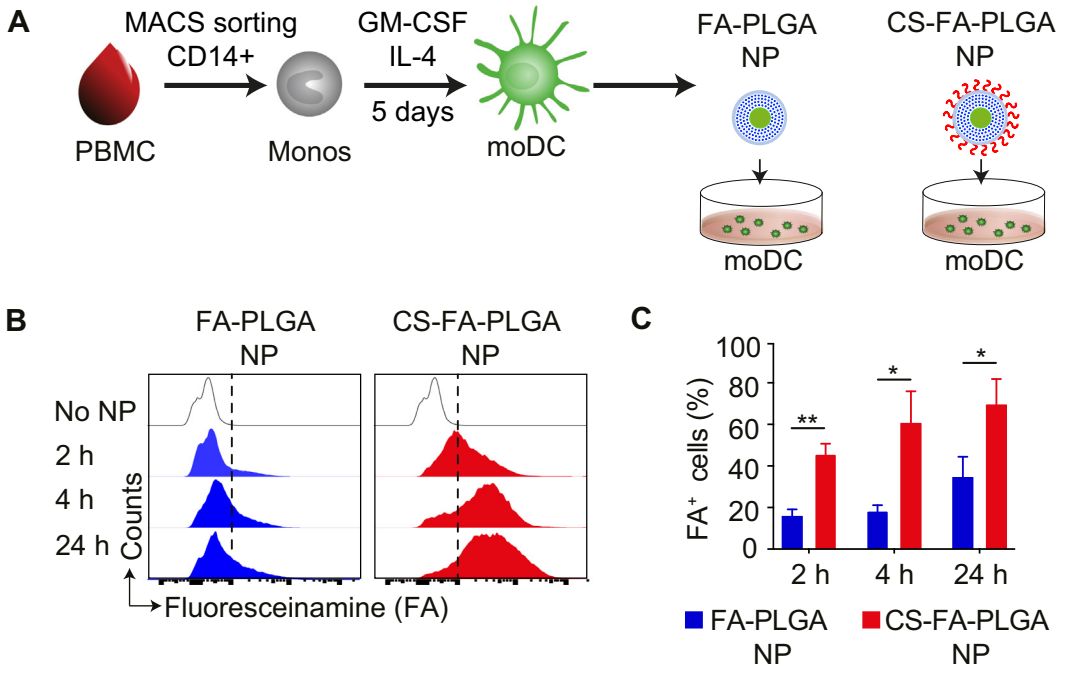

Figure 4. **CS-FA-PLGA nanoparticles are effectively internalized by human moDC. (A)** Monocytes were isolated from PBMC by magnetic activated cell sorting (MACS) for CD14+ cells, differentiated to monocyte-derived DC (moDC), and were then treated with FA-PLGA or CS-FA-PLGA NP. **(B)** moDC were treated with 60 μg/ml FA-PLGA or CS-FA-PLGA NP for 2, 4 and 24 h at 37 °C, and the percentage of FA positive cells was determined by flow cytometry. Representative data of moDC from one donor is shown. **(C)** Quantification of FA positive moDC from 5 donors. The error bars indicate mean ± SEM (two tailed Wilcoxon test, $^{**}P \leq 0.0015$, $^{*}P \leq 0.0309$, n = 5).

Treatment with FA-labeled PLGA or chitosan-coated PLGA nanoparticles does not induce upregulation of surface activation markers on moDC

In order to evaluate whether treatment with FA-PLGA or CS-FA-PLGA NP activate moDC, surface activation markers were analyzed by flow cytometry before and after 2, 4, and 24 h of NP treatment. Upon LPS treatment, moDC showed a 2.5-fold increased mean fluorescent intensity (MFI) of MHC-I expression when compared with non-treated moDC. In contrast, neither upon FA-PLGA nor CS-FA-PLGA NP treatment moDC showed significant MHC-I up-regulation. Similarly, CD11c, MHC-II, CD86, and CD40 were not up-regulated after FA-PLGA or CS-FA-PLGA NP treatment, whereas after LPS treatment the highest fold increase was detected after 24 h of incubation for CD11c and MHC-II (approx. 4-fold), CD86 (approx. 8-fold) and CD40 (approx. 7-fold). Interestingly, the mannose-receptor (MR) surface expression remained at basal levels after 24 h of incubation with FA-PLGA NP, whereas after exposure to CS-FA-PLGA NP it increased after 2 h of incubation, then decreased below basal levels after 4 h, and after 24 h of incubation it finally increased again by 2.5-fold (Figure 6, *A* and *B*). Thus, our results revealed that even after 24 h of incubation with FA-PLGA or CS-FA-PLGA NP there was no significant up-regulation of activation markers on the surface of moDC, except for the MR, which was differentially regulated upon CS-PLGA NP treatment.

Within moDC, FA-labeled chitosan-coated PLGA nanoparticles are preferentially delivered to early and late endosomes

To further study the intracellular localization after NP uptake, moDC were incubated for 2 h with FA-PLGA or CS-FA-PLGA NP, cells were fixed, markers for intracellular organelles were immunolabeled with specific antibodies, confocal microscopic analysis was performed, and colocalization between FA fluorescence derived from internalized NP and labeled subcellular compartments, as indicated by the Pearson's correlation coefficient (PCC), was analyzed. In these assays, Rab5a was used as a marker for early endosomes, which appear in early stages of endocytosis, whereas Rab7 was used to identify late endosomes, which develop after acidification of early endosomes (Figure 7, *A*). Upon treatment of moDC with FA-PLGA NP, a PCC with Rab5a and Rab7 of approx. 0.3 was detected, whereas upon treatment with CS-FA-PLGA NP a significantly enhanced value of approx. 0.5 was obtained. Interestingly, Lamp1 that was used as a marker for lysosomes, which are the most acidic organelle of cells, gave a PCC of approx. 0.4 with FA-PLGA NP, while with CS-FA-PLGA NP a value of 0.2 was obtained (Figure 7, *B* and *C*). Of note, although the FA fluorescence intensity diminishes with decreasing pH, both FA-PLGA and CS-FA-PLGA NP showed a very similar pH-dependent decline with residual fluorescence being detectable even after 2 h of exposure to acidic pH (Supplementary Figure 4), thus allowing the comparative analysis of FA-PLGA and CS-

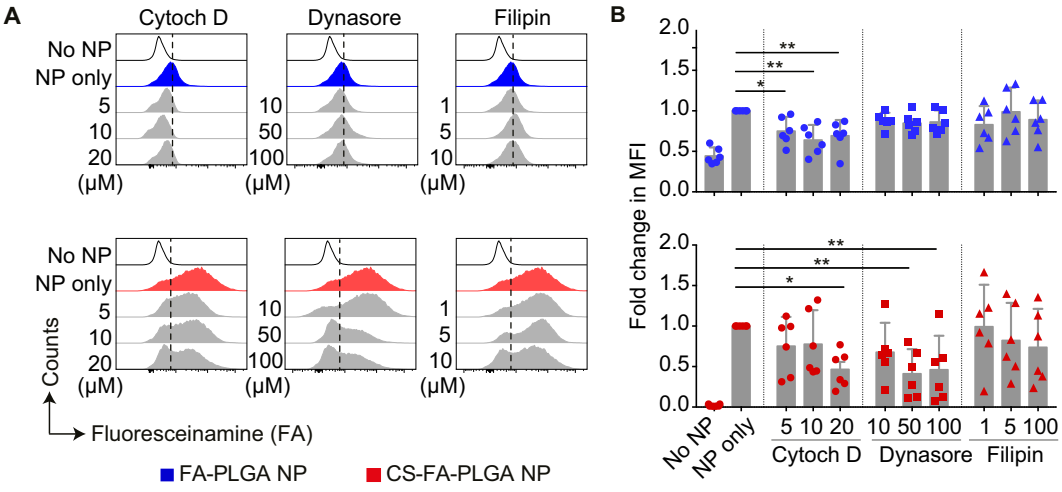

Figure 5. **FA-PLGA nanoparticles are primarily taken up by actin-dependent endocytosis, while CS-FA-PLGA nanoparticles enter moDC mainly by clathrin-mediated endocytosis.** moDC were incubated with increasing concentrations of the endocytosis inhibitors cytochalasin D, dynasore or filipin for 30 min at 37 °C. Cells were treated with 60 μg/ml of FA-PLGA or CS-FA-PLGA NP for 2 h and NP uptake was determined by flow cytometry. Results were normalized by setting the mean fluorescent intensity (MFI) of controls treated only with NP at 100% and calculating the fold-change in MFI of the other samples. The error bars indicate mean ± SEM (Friedman test $^{**}P \leq 0.0017$, $^{*}P \leq 0.0330$, n = 6).

FA-PLGA NP localization in acidic subcellular compartments. To identify recycling endosomes, the marker Rab11 was analyzed, which resulted in PCC values below 0.2 for both NP. This was also the case for BiP, which was used as a marker for the endoplasmic reticulum (ER), and for GM130, which is a marker for the Golgi bodies (Supplementary Figure 5). Thus, while both NP preparations colocalized similarly low with recycling endosomes, the ER, and Golgi bodies, CS-FA-PLGA NP showed a higher colocalization with early and late endosomes than FA-PLGA NP, which colocalized to a higher extent with lysosomes.

Discussion

Nanoparticulated delivery systems hold promise as innovative formulations to enhance efficacy and reduce adverse effects of new drugs. Drug delivery vehicles ideally should be able to target specific cells without inducing adverse reactions. Furthermore, an in-depth understanding of the interaction of nanoparticle formulations with human immune cells is of key relevance, as regardless of the application route that eventually will be chosen, such nanoparticle drug formulations will come in direct contact with blood or tissue-resident immune cells. Here we found that amongst PBMC, APC effectively internalize FA-PLGA and CS-FA-PLGA NP. In moDC, these NP caused low cytotoxic effects and they did not confer immunostimulatory effects. We additionally found that moDC show a preferential uptake of CS-FA-PLGA NP, which upon internalization are mostly delivered to early and late endosomes, presumably via receptor-mediated endocytosis.

PLGA and CS-PLGA NP were generated by using pharmaceutical grade excipients. Additionally, the raw materials as well as the final products were thoroughly tested for absence of LPS contaminations, which is of key relevance when assays with primary human immune cells are performed. NP generated under such conditions showed high quality, including absence of any detectable LPS contamination, as well as consistent physicochemical and morphological properties, even after addition of the FA fluorescent dye. Of note, FA labeling slightly decreased the ζ-potential of CS-PLGA NP. Since FA conjugation decreases the anionic charge of the PLGA core, and the attachment of chitosan is determined by electrostatic interactions, less chitosan is able to bind the core after FA conjugation and thus the ζ-potential of CS-FA-PLGA NP is reduced. Additionally, both NP had only minor toxic effects at concentrations below 100 μg/ml and only a moderate increase in cytotoxicity was observed at very high doses.

Therefore, we proceeded with experiments in human PBMC to assess the internalization of FA-PLGA and CS-FA-PLGA NP. We observed that despite the far more abundant presence of T cells, both NP were preferentially taken up by APC. Amongst APC, monocytes showed an even higher uptake of both NP preparations than DC. Presumably, this is due to the innate phagocytic function of APC, which is basically absent in lymphocytes. Interestingly, the kinetics of internalization in APC was much faster for CS-FA-PLGA than for FA-PLGA NP, as indicated by the more efficient uptake of CS-FA-PLGA after short incubation times. Such faster uptake kinetics are probably conferred by specific chitosan interactions with endocytic receptors that are expressed by APC[27] as well as by the electrostatic attraction caused by the positively charged chitosan and the negatively charged cell surface.[28] However, this still has to be experimentally addressed in greater detail. These traits could be exploited, e.g., during i.v. injection of CS-PLGA NP to selectively target recirculating APC within the blood, whereas upon i.m. injection of PLGA NP enhanced interaction times between the NP and the APC might be available in the draining lymph node, which might allow NP uptake independent of the functionalization with chitosan. Nevertheless, such strategies

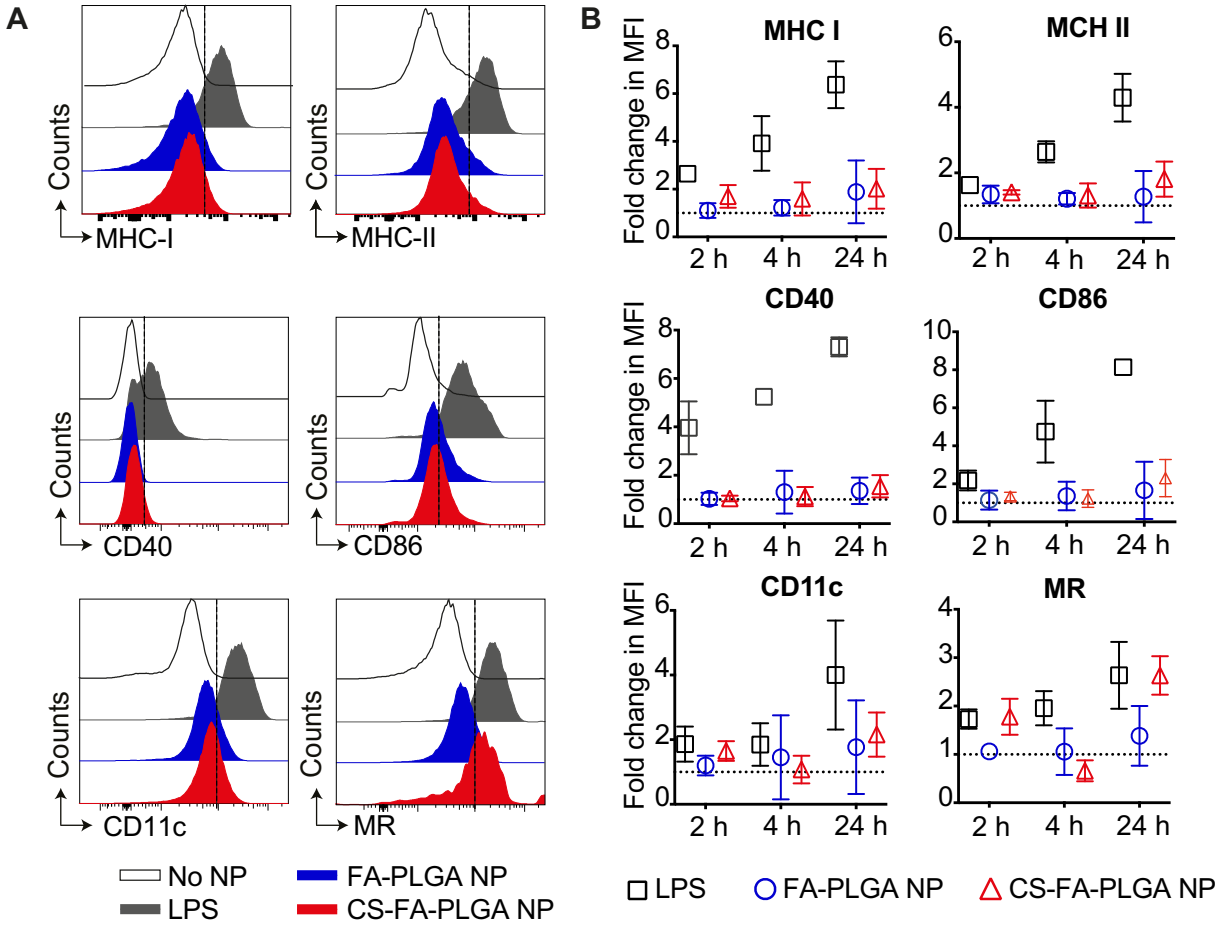

Figure 6. **Human moDC are not activated upon treatment with FA-PLGA or CS-FA-PLGA nanoparticle.** moDC prepared as described in Fig. 4 were treated with 60 μg/ml of FA-PLGA or CS-FA-PLGA NP at 37 °C for 2, 4 and 24 h, stained for surface activation markers and analyzed by flow cytometry. LPS (100 ng/ml) was used as a positive control. **(A)** Histograms correspond to surface expression of MHC-I, CD11c, MHC-II, CD86, mannose receptor (MR) and CD40 for one representative donor. **(B)** Values shown correspond to fold increase in MFI compared to basal conditions (no NP treatment). N = 5 from 3 independent experiments.

would have to be carefully studied in relevant animal models before applications in humans can be considered.

In addition, we observed a strong preference in the uptake of CS-FA-PLGA NP by moDC when compared with FA-PLGA NP. Beyond the electrostatic advantage that CS-FA-PLGA NP have over FA-PLGA NP, this can be explained by the fact that moDC show high expression of receptors involved in chitosan sensing. Amongst these, TLR2, Dectin-1 and the mannose receptor (MR)[29,30] play major roles and are known to enhance cellular uptake upon involvement.[31] In this context, chitosan functionalization of PLGA NP might promote receptor-mediated endocytosis, which is a clathrin-dependent process, and which seems to be more efficient than the non-specific uptake of non-functionalized PLGA NP. Indeed, our experiments indicated that in moDC the predominant uptake mechanism for CS-FA-PLGA NP is clathrin-dependent, while in the case of FA-PLGA NP macropinocytosis seems to be the main pathway.

As suspected from the consistent quality of both NP preparations, we did not observe any activation of moDC following FA-PLGA or CS-FA-PLGA NP treatment in moDC. Nevertheless, a slight regulation in the surface expression of the MR was observed upon treatment with CS-FA-PLGA NP. MR surface expression was first increased, then decreased and later increased again. These results are compatible with the hypothesis that the MR is the main receptor involved in the recognition of chitosan derivatives[32] and as it is an endocytic receptor, it is also internalized to endosomal compartments and further re-shuttled in its empty form back to the plasma membrane.[33] Of note, other studies have shown that the efficacy of DC-targeted delivery might be enhanced using natural ligands that bind DC-specific receptors, compared with approaches using specific antibodies. The strategy to use natural receptor ligands for NP functionalization promotes receptor recycling and thus, increases the rate of antigen internalization.[34]

Furthermore, we found that CS-FA-PLGA NP are mostly delivered to early and late endosomes, while non-functionalized FA-PLGA NP mostly end up in other subcellular compartments, such as lysosomes. This further points towards receptor-

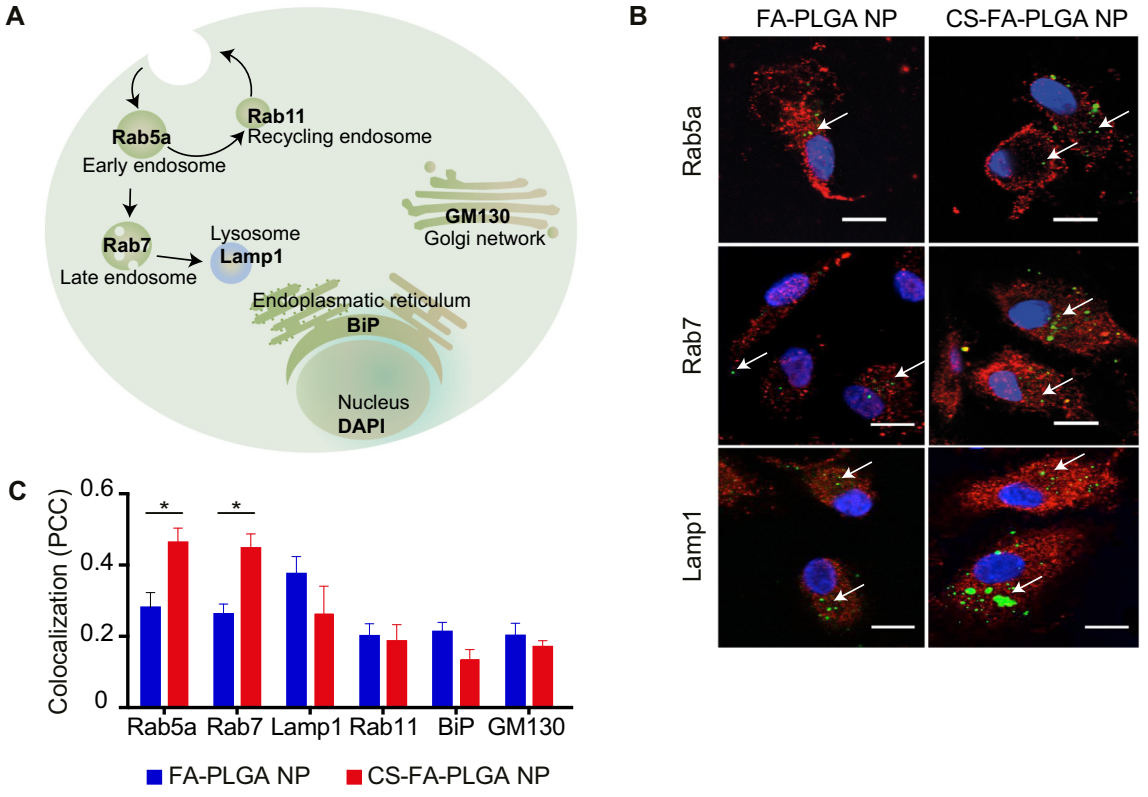

Figure 7. **CS-FA-PLGA nanoparticles are preferentially delivered to endosomal compartments in moDC. (A)** Schematic depiction of organelle-specific markers used to label cellular compartments within moDC (early endosomes (Rab5a), late endosomes (Rab7), lysosomes (Lamp1), recycling endosomes (Rab11), endoplasmatic reticulum (BiP), and Golgi bodies (GM130)). **(B)** Human moDC generated as described in Fig. 4 were treated with 60 μg/ml of FA-PLGA or CS-FA-PLGA NP for 2 h at 37 °C, fixed, and intracellular organelles were immunolabeled and counter-stained with an Alexa Fluor 647-coupled secondary antibody. DAPI staining was performed to identify the cell nuclei and samples were analyzed by confocal microscopy. Scale bar represents 1 μm. **(C)** Pearson's correlation coefficient (PCC) between organelle markers and FA-fluorescence derived from CS-FA-PLGA or FA-PLGA NP. For each donor a minimum of 3 photos was analyzed, each image comprising 5–10 cells. The error bars indicate mean ± SD (two-way ANOVA $*P \leq 0.033$, N = 3 donors from 2 independent experiments).

mediated endocytosis of CS-FA-PLGA NP, as it has been proven that recognition via the above-mentioned receptors mediates delivery into endosomal compartments via a tyrosine-based motif in the receptor cytoplasmic tail.[35,36]

Interestingly, moDC showed a higher uptake of CS-FA-PLGA NP than DC within PBMC. As in vitro generated moDC resemble DC generated under inflammatory conditions in vivo, they are known to have a higher endocytic capacity as well as higher expression of surface receptors such as the MR, in comparison to steady-state DC found in blood.[37,38] Additionally, monocytes and DC within PBMC might intrinsically compete for the uptake of NP. Despite the fact that both cell types are considered professional phagocytes, DC are also specialized in activating T cells and initiating an adaptive immune response, whereas the primary function of most phagocytes is mainly to destroy foreign particles.[39] Thus, when treating PBMC with either NP preparation, uptake by monocytes might outpace uptake by DC resulting in the reduced NP internalization we observed in DC from PBMC when compared with moDC.

Overall, these results demonstrate that CS-PLGA NP are particularly for antigen delivery to APC, e.g., to induce antigen presentation to lymphocytes or to modulate APC function. Along this line, several studies have demonstrated that targeting antigens to DC via the MR enhances uptake as well as antigen presentation by MHC-I and MHC-II molecules.[40] This could be relevant for antigen-specific vaccination[41] as well as for the induction of tolerance.[42,43] Furthermore, many viral and bacterial pathogens preferentially infect APC.[44] This has been demonstrated for some of the most threatening pathogens such as Dengue virus, HIV and *Mycobacterium tuberculosis*, which successfully evade immune responses mainly by hiding and persisting in endosomal compartments.[45] Thus, it is conceivable that CS-PLGA NP formulations of antibiotics or antivirals will turn out to be efficacious for the treatment of such global threats.

Appendix A. Supplementary data

Supplementary data to this article can be found online at https://doi.org/10.1016/j.nano.2019.102073.

References

1. Senapati S, Mahanta AK, Kumar S, Maiti P. Controlled drug delivery vehicles for cancer treatment and their performance. *Signal Transduct Target Ther* 2018;**3**:7, https://doi.org/10.1038/s41392-017-0004-3.

2. Getts DR, Shea LD, Miller SD, King NJ. Harnessing nanoparticles for immune modulation. *Trends Immunol* 2015;**36**:419-27, https://doi.org/10.1016/j.it.2015.05.007.
3. Du J, Zhang YS, Hobson D, Hydbring P. Nanoparticles for immune system targeting. *Drug Discov Today* 2017;**22**:1295-301, https://doi.org/10.1016/j.drudis.2017.03.013.
4. Sussman E, Clark M and Shastri VP. Functionalized polymeric nanoparticles. MRS Proceedings 2011; 818: M12.9.1. DOI: 10.1557/proc-818-m12.9.1.
5. Gregory AE, Titball R, Williamson D. Vaccine delivery using nanoparticles. *Front Cell Infect Microbiol* 2013;**3**:13, https://doi.org/10.3389/fcimb.2013.00013.
6. Hartshorn CM, Bradbury MS, Lanza GM, Nel AE, Rao J, Wang AZ, et al. Nanotechnology strategies to advance outcomes in clinical Cancer care. *ACS Nano* 2018;**12**:24-43, https://doi.org/10.1021/acsnano.7b05108.
7. Wong JKL, Mohseni R, Hamidieh AA, MacLaren RE, Habib N, Seifalian AM. Will nanotechnology bring new Hope for gene delivery? *Trends Biotechnol* 2017;**35**:434-51, https://doi.org/10.1016/j.tibtech.2016.12.009.
8. Schmid D, Park CG, Hartl CA, Subedi N, Cartwright AN, Puerto RB, et al. T cell-targeting nanoparticles focus delivery of immunotherapy to improve antitumor immunity. *Nat Commun* 2017;**8**:1747, https://doi.org/10.1038/s41467-017-01830-8.
9. Parveen S, Misra R, Sahoo SK. Nanoparticles: a boon to drug delivery, therapeutics, diagnostics and imaging. *Nanomedicine* 2012;**8**:147-66, https://doi.org/10.1016/j.nano.2011.05.016.
10. Oberdorster G. Safety assessment for nanotechnology and nanomedicine: concepts of nanotoxicology. *J Intern Med* 2010;**267**:89-105, https://doi.org/10.1111/j.1365-2796.2009.02187.x.
11. Kononenko V, Narat M, Drobne D. Nanoparticle interaction with the immune system. *Arh Hig Rada Toksikol* 2015;**66**:97-108, https://doi.org/10.1515/aiht-2015-66-2582.
12. Zolnik BS, Gonzalez-Fernandez A, Sadrieh N, Dobrovolskaia MA. Nanoparticles and the immune system. *Endocrinology* 2010;**151**:458-65, https://doi.org/10.1210/en.2009-1082.
13. Dobrovolskaia MA, Shurin M, Shvedova AA. Current understanding of interactions between nanoparticles and the immune system. *Toxicol Appl Pharmacol* 2016;**299**:78-89, https://doi.org/10.1016/j.taap.2015.12.022.
14. Ravi Kumar MNV, Bakowsky U, Lehr CM. Preparation and characterization of cationic PLGA nanospheres as DNA carriers. *Biomaterials* 2004;**25**:1771-7, https://doi.org/10.1016/j.biomaterials.2003.08.069.
15. Mittal A, Raber AS, Schaefer UF, Weissmann S, Ebensen T, Schulze K, et al. Non-invasive delivery of nanoparticles to hair follicles: a perspective for transcutaneous immunization. *Vaccine* 2013;**31**:3442-51, https://doi.org/10.1016/j.vaccine.2012.12.048.
16. Jayakumar R, Nwe N, Tokura S, Tamura H. Sulfated chitin and chitosan as novel biomaterials. *Int J Biol Macromol* 2007;**40**:175-81, https://doi.org/10.1016/j.ijbiomac.2006.06.021.
17. Makadia HK, Siegel SJ. Poly lactic-co-glycolic acid (PLGA) as biodegradable controlled drug delivery carrier. *Polymers* 2011;**3**:1377-97, https://doi.org/10.3390/polym3031377.
18. Mittal A, Schulze K, Ebensen T, Weissmann S, Hansen S, Lehr CM, et al. Efficient nanoparticle-mediated needle-free transcutaneous vaccination via hair follicles requires adjuvantation. *Nanomedicine* 2015;**11**:147-54, https://doi.org/10.1016/j.nano.2014.08.009.
19. Haque AKMA, Dewerth A, Antony JS, Riethmüller J, Latifi N, Yasar H, et al. Modified hCFTR mRNA restores normal lung function in a mouse model of cystic fibrosis. *bioRxiv* 2017. 202853. DOI: https://doi.org/10.1101/202853.
20. Mahiny AJ, Dewerth A, Mays LE, Alkhaled M, Mothes B, Malaeksefat E, et al. In vivo genome editing using nuclease-encoding mRNA corrects SP-B deficiency. *Nature Biotechnol* 2015;**33**:584, https://doi.org/10.1038/nbt.3241.
21. Zupancic E, Curato C, Paisana M, Rodrigues C, Porat Z, Viana AS, et al. Rational design of nanoparticles towards targeting antigen-presenting cells and improved T cell priming. *J Control Release* 2017;**258**:182-95, https://doi.org/10.1016/j.jconrel.2017.05.014.
22. Weiss B, Schaefer UF, Zapp J, Lamprecht A, Stallmach A, Lehr CM. Nanoparticles made of fluorescence-labelled poly(L-lactide-co-glycolide): preparation, stability, and biocompatibility. *J Nanosci Nanotechnol* 2006;**6**:3048-56, https://doi.org/10.1166/jnn.2006.424.
23. Yasar H, Biehl A, De Rossi C, Koch M, Murgia X, Loretz B, et al. Kinetics of mRNA delivery and protein translation in dendritic cells using lipid-coated PLGA nanoparticles. *J Nanobiotechnology* 2018;**16**:72, https://doi.org/10.1186/s12951-018-0401-y.
24. Mortensen K, Larsson L-I. Effects of cytochalasin D on the actin cytoskeleton: association of neoformed actin aggregates with proteins involved in signaling and endocytosis. *Cell Mol Life Sci* 2003;**60**:1007-12, https://doi.org/10.1007/s00018-003-3022-x.
25. Macia E, Ehrlich M, Massol R, Boucrot E, Brunner C, Kirchhausen T. Dynasore, a cell-permeable inhibitor of dynamin. *Dev Cell* 2006;**10**:839-50, https://doi.org/10.1016/j.devcel.2006.04.002.
26. Nabi IR, Le PU. Caveolae/raft-dependent endocytosis. *J Cell Biol* 2003;**161**:673, https://doi.org/10.1083/jcb.200302028.
27. Dumitriu S. *Polymeric Biomaterials, Revised and Expanded*. 2nd ed. Boca Raton: CRC Press; 2001.
28. Lee DW, Lim H, Chong HN, Shim WS. Advances in chitosan material and its hybrid derivatives: a review. *Open Biomater J* 2009;**1**:10-20, https://doi.org/10.2174/1876502500901010010.
29. Bueter CL, Specht CA, Levitz SM. Innate sensing of chitin and chitosan. *PLoS Pathog* 2013;**9**e1003080, https://doi.org/10.1371/journal.ppat.1003080.
30. van Kooyk Y. C-type lectins on dendritic cells: key modulators for the induction of immune responses. *Biochem Soc Trans* 2008;**36**:1478-81, https://doi.org/10.1042/BST0361478.
31. Kerrigan AM, Brown GD. C-type lectins and phagocytosis. *Immunobiology* 2009;**214**:562-75, https://doi.org/10.1016/j.imbio.2008.11.003.
32. Han Y, Zhao L, Yu Z, Feng J, Yu Q. Role of mannose receptor in oligochitosan-mediated stimulation of macrophage function. *Int Immunopharmacol* 2005;**5**:1533-42, https://doi.org/10.1016/j.intimp.2005.04.015.
33. Taylor PR, Gordon S, Martinez-Pomares L. The mannose receptor: linking homeostasis and immunity through sugar recognition. *Trends Immunol* 2005;**26**:104-10, https://doi.org/10.1016/j.it.2004.12.001.
34. Tacken PJ, Ter Huurne M, Torensma R, Figdor CG. Antibodies and carbohydrate ligands binding to DC-SIGN differentially modulate receptor trafficking. *Eur J Immunol* 2012;**42**:1989-98, https://doi.org/10.1002/eji.201142258.
35. Burgdorf S, Kurts C. Endocytosis mechanisms and the cell biology of antigen presentation. *Curr Opin Immunol* 2008;**20**:89-95, https://doi.org/10.1016/j.coi.2007.12.002.
36. Moseman AP, Moseman EA, Schworer S, Smirnova I, Volkova T, von Andrian U, et al. Mannose receptor 1 mediates cellular uptake and endosomal delivery of CpG-motif containing oligodeoxynucleotides. *J Immunol* 2013;**191**:5615-24, https://doi.org/10.4049/jimmunol.1301438.
37. Segura E, Amigorena S. Inflammatory dendritic cells in mice and humans. *Trends Immunol* 2013;**34**:440-5, https://doi.org/10.1016/j.it.2013.06.001.
38. Min J, Yang D, Kim M, Haam K, Yoo A, Choi JH, et al. Inflammation induces two types of inflammatory dendritic cells in inflamed lymph nodes. *Exp Mol Med* 2018;**50**:e458, https://doi.org/10.1038/emm.2017.292.
39. Savina A, Amigorena S. Phagocytosis and antigen presentation in dendritic cells. *Immunol Rev* 2007;**219**:143-56, https://doi.org/10.1111/j.1600-065X.2007.00552.x.
40. Tacken PJ, de Vries IJ, Torensma R, Figdor CG. Dendritic-cell immunotherapy: from ex vivo loading to in vivo targeting. *Nat Rev Immunol* 2007;**7**:790-802, https://doi.org/10.1038/nri2173.
41. Lambricht L, Peres C, Florindo H, Préat V, Vandermeulen G. In: Skwarczynski M, Toth I, editors. *Polymer-Based Nanoparticles as Modern Vaccine Delivery Systems*. William Andrew Publishing; 2017. p. 185-203. Micro and Nanotechnology in Vaccine Development.

42. Klippstein R, Pozo D. Nanotechnology-based manipulation of dendritic cells for enhanced immunotherapy strategies. *Nanomedicine* 2010;**6**:523-9, https://doi.org/10.1016/j.nano.2010.01.001.
43. Kishimoto TK, Maldonado RA. Nanoparticles for the induction of antigen-specific immunological tolerance. *Front Immunol* 2018;**9**:230, https://doi.org/10.3389/fimmu.2018.00230.
44. Unanue ER. Intracellular pathogens and antigen presentation-new challenges with legionella pneumophila. *Immunity* 2003;**18**:722-4, https://doi.org/10.1016/S1074-7613(03)00145-6.
45. Khan N, Gowthaman U, Pahari S, Agrewala JN. Manipulation of costimulatory molecules by intracellular pathogens: veni, vidi, vici!! *PLoS Pathog* 2012;**8**e1002676, https://doi.org/10.1371/journal.ppat.1002676.